Optica Applicata, Vol. XLVII, No. 2, 2017
DOI: 10.5277/oa170213

Phase and group velocities of surface waves in left-handed material waveguide structures

SOFYAN A. TAYA*, KHITAM Y. ELWASIFE, IBRAHIM M. QADOURA

Physics Department, Islamic University of Gaza, Gaza, Palestine

*Corresponding author: staya@iugaza.edu.ps

We assume a three-layer waveguide structure consisting of a dielectric core layer embedded between two left-handed material claddings. The phase and group velocities of surface waves supported by the waveguide structure are investigated. Many interesting features were observed such as normal dispersion behavior in which the effective index increases with the increase in the propagating wave frequency. The phase velocity shows a strong dependence on the wave frequency and decreases with increasing the frequency. It can be enhanced with the increase in the guiding layer thickness. The group velocity peaks at some value of the normalized frequency and then decays.

Keywords: slab waveguide, phase velocity, group velocity, left-handed materials.

1. Introduction

Materials with negative electric permittivity ε and magnetic permeability μ are artificially fabricated metamaterials having certain peculiar properties which cannot be found in natural materials. The unusual properties include negative refractive index, reversed Goos–Hänchen shift, reversed Doppler shift, and reversed Cherenkov radiation. These materials are known as left-handed materials (LHMs) since the electric field, magnetic field, and the wavevector form a left-handed set. VESELAGO was the first who investigated the propagation of electromagnetic waves in such media and predicted a number of unusual properties [1]. Till now, LHMs have been realized successfully in microwaves, terahertz waves and optical waves. The slab waveguides comprising LHM layer have been discussed extensively and many papers have been published [2–34]. PENDRY *et al*. proposed a mechanism for depression of the plasma frequency into the far infrared or even gigahertz band [2] and he also proposed an unconventional lens [3] using LHM. PENDRY found that a slab of LHM can focus all Fourier components of a 2D image. The characteristic equation of the surface polaritons of a LHM slab was studied [4]. A theoretical analysis of the radiation from a traveling-wave infinitely-extent sheet of monochromatic electric current that is placed at the interface between a traditional dielectric and a LHM is presented [5]. SHELBY *et al*. investigated experimentally the transmission from a 2D isotropic LHM [6]. A theoretical analysis of a slab of LHM and the

possibility of acting as a phase compensator/conjugator were investigated [7]. MAHMOUD and VIITANEN studied the properties of surface wave modes in a grounded LHM slab [8]. It is demonstrated experimentally that a tunable negative permeability metamaterial can be obtained at microwave frequencies by introducing YIG rods into a periodic array of split ring resonators [9]. Multilayer LHM slab waveguide was studied and the dispersion relation was derived [10, 11]. The influence of negative-index layer on dispersion and power flow was investigated. Three normalized parameters (a, b, and V) were utilized to investigate the dispersion properties of different slab waveguide structures containing at least one LHM layer [12–14]. A symplectic finite-difference time-domain (SFDTD) technique was utilized for the first time to investigate the electromagnetic properties of LHMs [15]. A wave-absorber model containing air/LHM/RHM/metal structure was investigated [16]. The properties of wave-absorber were theoretically analyzed and simulated and the structure parameters were optimized employing a genetic algorithm [16]. Guided modes carried by a three layer metal-clad waveguide structure having LHM core layer were studied [17]. The dispersion properties of both transverse electric and transverse magnetic waves were analyzed [17]. The properties of waves guided in a structure comprising a LHM cladding and an anisotropic core layer were studied [18]. The dispersion properties showed a crucial dependence on the LHM parameters for $\omega > 5.2$ GHz. The surface polaritons excited at the interfaces of different waveguide structures comprising LHMs were derived, plotted and discussed [19]. It was shown that semiconductor nano-structures made from non-magnetic InAs/GaAs nano-rings can behave like a LHM in a certain optical frequency range [20]. The generation of the energy stream loops for the evanescent field around the interfaces of a LHM slab has been investigated with a finite-difference time -domain technique [21]. Asymmetric three-layer LHM slab waveguide structure was investigated and the field distribution was analyzed in details [22]. The reflection and transmission through a dielectric slab surrounded by two LHM media were presented [23]. Lorentz and Drude medium models for the dispersion of LHM were considered. It was observed that damping frequency has an ignorable effect on the reflectance. A wide band filter based on LHM theory was proposed [24]. The length of the main part is only 1/20 compared to the working wavelength. It can be used to eliminate the noise in RF interconnect and other fields. It was shown that a linearly polarized beam can experience either a negative or a positive Goos–Hänchen shift when totally reflected from a LHM [25]. The dispersion properties of lossy, dispersive, and anisotropic LHM were investigated and the possible use of the structure as a refractometric sensor was discussed [26–29]. Among the wide range of applications, slab waveguide sensing was one of the possible applications of LHMs [30–34].

The aim of this work is to investigate the peculiar features of surface waves that propagate along the interfaces of a dielectric slab bounded by two LHM layers. To the best of our knowledge, the structure of LHM/dielectric/LHM has not been investigated in the literature.

In this work, we investigate the phase and group velocities of surface waves excited at the interface of dielectric and LHM.

2. Phase and group velocities

The structural setup of interest is a dielectric slab of thickness d sandwiched between two LHMs as a cladding and substrate. Both cladding and substrate are considered to be semi-infinite, dispersive, lossless, homogeneous and isotropic LHM. The geometry of the structure under study is shown in Fig. 1.

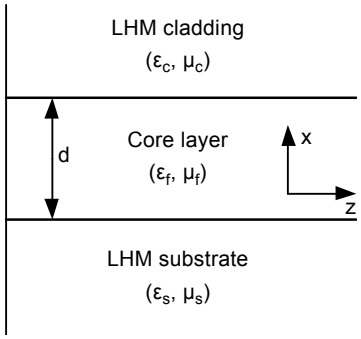

Fig. 1. Schematic diagram of a dielectric slab surrounded by left-handed media.

The propagation of an electromagnetic wave is considered along the z-axis. The LHM is described by a negative permittivity $\varepsilon(\omega)$ and permeability $\mu(\omega)$ that given by

$$\varepsilon_{\mathrm{c,\,s}}(\omega) = 1 - \frac{\omega_{\mathrm{p}}^2}{\omega^2} \tag{1}$$

$$\mu_{\mathrm{c,\,s}}(\omega) = 1 - \frac{F\omega^2}{\omega^2 - \omega_0^2} \tag{2}$$

where ω_{p} is plasma frequency, ω_0 is the characteristic frequency of LHM and subscripts c, s represent cladding and substrate, respectively. The parameters of the LHM are taken as $\omega_{\mathrm{p}} = 10$ GHz, $\omega_0 = 4$ GHz and parameter $F = 0.56$. We first consider TE modes in which the following field components E_y, H_x, and H_z exist. In the region of LHM substrate, we have

$$E_y(x) = \exp(k_{\mathrm{s}} x) \tag{3}$$

$$H_x(x) = -\frac{k_z}{k_0 \mu_{\mathrm{s}}} \exp(k_{\mathrm{s}} x) \tag{4}$$

$$H_z(x) = -\frac{ik_{\mathrm{s}}}{k_0 \mu_{\mathrm{s}}} \exp(k_{\mathrm{s}} x) \tag{5}$$

where $k_{\mathrm{s}} = \sqrt{k_z^2 - k_0^2 \varepsilon_{\mathrm{s}} \mu_{\mathrm{s}}}$.

In the cladding region ($x > d$), the field components can be written as

$$E_y(x) = E_0 \exp(-k_c x) \tag{6}$$

$$H_x(x) = -\frac{E_0 k_z}{k_0 \mu_c} \exp(-k_c x) \tag{7}$$

$$H_z(x) = \frac{i E_0 k_c}{k_0 \mu_c} \exp(-k_c x) \tag{8}$$

where E_0 is the wave amplitude, and $k_c = \sqrt{k_z^2 - k_0^2 \varepsilon_c \mu_c}$.

In the dielectric core layer, the nonzero field components are given by

$$E_y(x) = C_1 \exp(k_f x) + C_2 \exp(-k_f x) \tag{9}$$

$$H_x(x) = -\frac{k_z}{k_0 \mu_f}\left[C_1 \exp(k_f x) + C_2 \exp(-k_f x)\right] \tag{10}$$

$$H_z(x) = -\frac{i k_f}{k_0 \mu_f}\left[C_1 \exp(k_f x) - C_2 \exp(-k_f x)\right] \tag{11}$$

where C_1 and C_2 represent wave field constant, and $k_f = \sqrt{k_z^2 - k_0^2 \varepsilon_f \mu_f}$.

Applying the boundary conditions such that E_y and H_z are continuous at $z = 0$ and $z = d$, we obtain

$$\tanh(k_f d) = \frac{\mu_c \mu_f k_c k_f + \mu_s \mu_f k_c k_f}{\mu_s \mu_c k_f^2 - \mu_f^2 k_s k_c} \tag{12}$$

If we consider symmetric waveguide in which the cladding and substrate are identical, $\mu_c = \mu_s$ and $\varepsilon_c = \varepsilon_s$, Eq. (12) becomes

$$\tanh(k_f d) = \frac{\mu_c \mu_f k_c k_f + \mu_c \mu_f k_s k_f}{\mu_c^2 k_f^2 - \mu_f^2 k_s k_c} \tag{13}$$

Equation (13) represents the dispersion relation for TE surface waves. The numerical solution of Eq. (13) gives the effective refractive index of the TE surface mode for a given frequency.

The group velocity for TE electromagnetic surface waves is given by $v_g = \mathrm{d}\omega/\mathrm{d}k_x$. Differentiating the dispersion relation given by Eq. (13) with respect to ω, we get after a tedious derivation and mathematical manipulation

$$v_g = \frac{\mathrm{d}\omega}{\mathrm{d}k_x} = \frac{2\alpha_1 + \alpha_2}{\alpha_3 - 2\alpha_4} \tag{14}$$

where,

$$\alpha_1 = \frac{\mu_c k_f \alpha_5 + \mu_f k_c \alpha_6}{\mu_c^2 k_f^2 + \mu_f^2 k_c^2}$$

$$\alpha_2 = \frac{dk_x}{k_f}$$

$$\alpha_3 = \frac{d}{k_f}\frac{\omega}{c^2}\varepsilon_f \mu_f$$

$$\alpha_4 = \frac{-\mu_c k_f \alpha_7 + \mu_c k_f \alpha_8 + \mu_c k_f \alpha_9 - \mu_f k_c \alpha_{10} - \mu_f k_c \alpha_{11}}{\mu_c^2 k_f^2 + \mu_f^2 k_c^2}$$

$$\alpha_5 = \frac{\mu_f k_x}{k_c}$$

$$\alpha_6 = \frac{\mu_c k_x}{k_f}$$

$$\alpha_7 = \frac{\mu_f}{k_c}\frac{\omega}{c^2}$$

$$\alpha_8 = \frac{\mu_f}{k_c}\frac{F}{c^2}\frac{\omega^5 - 2\omega_0^2\omega^3}{(\omega^2 - \omega_0^2)^2}$$

$$\alpha_9 = \frac{\mu_f}{k_c}\frac{F\omega_p^2}{c^2}\frac{\omega\omega_0^2}{(\omega^2 - \omega_0^2)^2}$$

$$\alpha_{10} = \frac{\mu_c}{k_f}\frac{\omega}{c^2}\varepsilon_f \mu_f$$

$$\alpha_{11} = \frac{2k_f F\omega\omega_0^2}{(\omega^2 - \omega_0^2)^2}$$

For TM polarized light, in the substrate layers, the nonzero field components are given by,

$$H_y(x) = \exp(k_s x) \tag{15}$$

$$E_x(x) = \frac{k_z}{k_0 \varepsilon_s}\exp(k_s x) \tag{16}$$

$$E_z(x) = \frac{ik_s}{k_0 \varepsilon_s} \exp(k_s x) \tag{17}$$

whereas in the cladding region ($x > d$), we can write

$$H_y(x) = H_0 \exp(-k_c x) \tag{18}$$

$$E_x(x) = \frac{H_0 k_z}{k_0 \varepsilon_c} \exp(-k_c x) \tag{19}$$

$$E_z(x) = -\frac{iH_0 k_c}{k_0 \varepsilon_c} \exp(-k_c x) \tag{20}$$

where H_0 is the wave amplitude.

The magnetic field and nonzero components of the electric field in the core layer can be written as

$$H_y(x) = C_1 \exp(k_f x) + C_2 \exp(-k_f x) \tag{21}$$

$$E_x(x) = \frac{k_z}{k_0 \varepsilon_f} \left[C_1 \exp(k_f x) + C_2 \exp(-k_f x) \right] \tag{22}$$

$$E_z(x) = \frac{ik_f}{k_0 \varepsilon_f} \left[C_1 \exp(k_f x) - C_2 \exp(-k_f x) \right] \tag{23}$$

For TM mode, the dispersion relation is given by

$$\tanh(k_f d) = \frac{\varepsilon_c \varepsilon_f k_s k_f + \varepsilon_s \varepsilon_f k_s k_f}{\varepsilon_s \varepsilon_c k_f^2 - \mu_f^2 k_s k_c} \tag{24}$$

Equation (24) gives the dispersion relation for TM surface waves. The numerical solution of Eq. (24) gives the effective refractive index of the TM surface mode for a given frequency.

Similarly, by differentiating Eq. (24) with respect to ω, we get the group velocity for TM mode as

$$v_g = \frac{d\omega}{dk_x} = \frac{2\beta_1 + \beta_2}{\beta_3 - 2\beta_4} \tag{25}$$

where,

$$\beta_1 = \frac{\varepsilon_c k_f \beta_5 + \varepsilon_f k_c \beta_6}{\varepsilon_c^2 k_f^2 + \varepsilon_f^2 k_c^2}$$

$$\beta_2 = \frac{dk_x}{k_f}$$

$$\beta_3 = \frac{d}{k_\mathrm{f}} \frac{\omega}{c^2} \varepsilon_\mathrm{f} \mu_\mathrm{f}$$

$$\beta_4 = \frac{\varepsilon_\mathrm{c} k_\mathrm{f} \beta_7 - \varepsilon_\mathrm{f} k_\mathrm{c} \beta_8}{\varepsilon_\mathrm{c}^2 k_\mathrm{f}^2 + \varepsilon_\mathrm{f}^2 k_\mathrm{c}^2}$$

$$\beta_5 = \frac{\varepsilon_\mathrm{f} k_x}{k_\mathrm{c}}$$

$$\beta_6 = \frac{\varepsilon_\mathrm{c} k_x}{k_\mathrm{f}}$$

$$\beta_7 = -\frac{\varepsilon_\mathrm{f}}{k_\mathrm{c}} \frac{\omega}{c^2} + \frac{\varepsilon_\mathrm{f}}{k_\mathrm{c}} \frac{F}{c^2} \frac{\omega^5 - 2\omega_0^2 \omega^3}{(\omega^2 - \omega_0^2)^2} + \frac{\varepsilon_\mathrm{f}}{k_\mathrm{c}} \frac{F\omega_\mathrm{p}^2}{c^2} \frac{\omega \omega_0^2}{(\omega^2 - \omega_0^2)^2}$$

$$\beta_8 = \frac{\varepsilon_\mathrm{c}}{k_\mathrm{f}} \frac{\omega}{c^2} \varepsilon_\mathrm{f} \mu_\mathrm{f} + \frac{2\omega_\mathrm{p}^2}{k_\mathrm{f} \omega^3}$$

3. Numerical results

Figure 1 shows a schematic diagram of the waveguide consisting of a dielectric core layer and two identical LHM claddings. The LHM parameters are commonly taken with the aid of experimentally obtained values: $\omega_0 = 4$ GHz, $\omega_\mathrm{p} = 10$ GHz, and $F = 0.56$. The dielectric core layer has the parameters: $\varepsilon_\mathrm{f} = 2.25$ and $\mu_\mathrm{f} = 1$. Surface waves are obtained in the narrow band of $4.67 \le \omega \le 4.717$ for TE waves and a wider band of $4.82 \le \omega \le 5.48$ for TM waves. In these bands, k_f is found to be pure imaginary. Using the above parameters, the dispersion relation was solved numerically for the effective refractive index of the guided mode. The dispersion properties can be investigated from

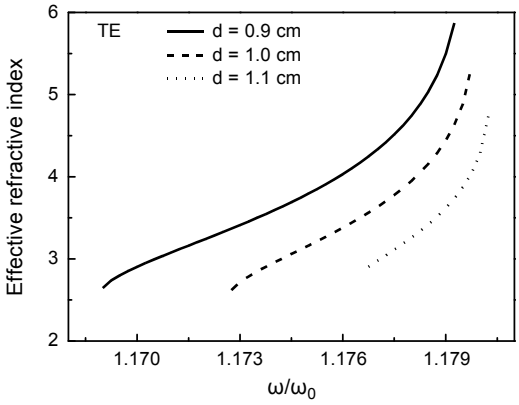

Fig. 2. Effective refractive index *vs.* ω/ω_0 for different values of core layer thickness (TE).

the dispersion curves which show the dependence of the longitudinal propagation constant k_z or the modal index of refraction on the guided wave frequency. The dispersion curves of surface waves are illustrated in Fig. 2 for different values of the core layer thickness. The figure reveals a normal dispersion property in which the effective index increases with the increase in the propagating wave frequency. The figure reflects a set of interesting features. First, as the core layer decreases, the dispersion curves move up showing an enhancement in the effective refractive index. Second, the operating frequency range becomes wider as the thickness of the core layer decreases. For $d = 0.9$ cm, the operating frequency range is 1.169 GHz $\leq \omega/\omega_0 \leq$ 1.17925 GHz, whereas for $d = 1$ cm, the range is 1.17275 GHz $\leq \omega/\omega_0 \leq$ 1.17975 GHz. For $d = 1.1$ cm, the range becomes 1.17675 GHz $\leq \omega/\omega_0 \leq$ 1.18025 GHz. This is an important feature which means that the core layer thickness can be adjusted to broaden or narrow the operating bands and modify the effective index to a desirable value. Figure 3 shows the dispersion curves for TM modes. The operating frequency band for TM surface waves is much wider than that of TE surface waves. Moreover, this band is crucially dependent on the core layer thickness. As the core layer thickness decreases, the dispersion curves move up showing an increase in the effective index.

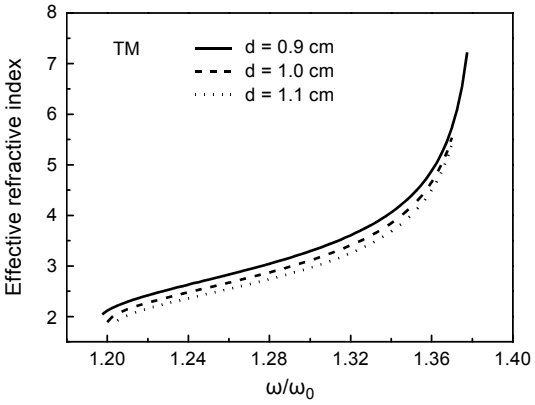

Fig. 3. Effective refractive index *vs.* ω/ω_0 for different values of core layer thickness (TM).

We now turn our attention to the phase and group velocities of surface waves in the proposed structure. The phase velocity is given by $v_{ph} = \omega/k_z$ for the surface TE and TM waves.

When the dispersion relations are solved numerically for the effective refractive index N, the longitudinal component of the wave number k_z is calculated as $k_z = k_0 N$, where $k_0 = \omega/c$ is the free space wave number. The phase velocity can be calculated as $v_{ph} = \omega/k_z$.

The dependence of the normalized phase velocity v_{ph}/c (where c is the speed of light in free space) on the normalized frequency ω/ω_0 for different core layer thickness is shown in Fig. 4. The figure reveals that the phase velocity of surface TE wave is

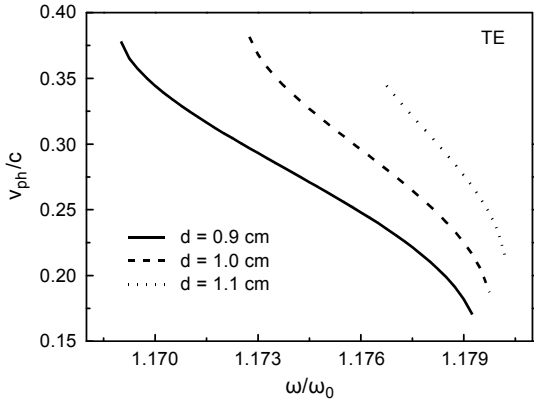

Fig. 4. Phase velocity of surface waves *vs.* ω/ω_0 (TE) for different values of thickness of the guiding layer.

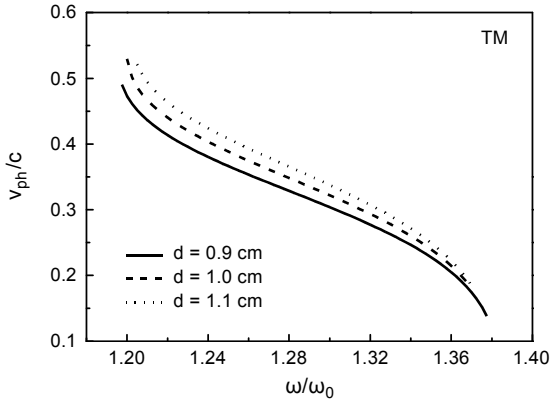

Fig. 5. Phase velocity of surface waves *vs.* ω/ω_0 (TM) for different values of thickness of the guiding layer.

slow and it shows strong dependence on the wave frequency, especially for a large value of d. The phase velocity decreases with increasing the frequency. When the thickness of the core layer is enhanced, the phase velocity is also enhanced. The phase velocity of surface TM waves *vs.* the normalized frequency is shown in Fig. 5. The curves show a less dependence on the frequency than TE. With the increase in the core thickness, the phase velocity reveals an enhancement. The group velocity of the wave is given by $v_{gz} = \partial\omega/\partial k_z$. The dependence of group velocity on normalized frequency is shown in Fig. 6 for different values of the core thickness. Group velocity increases as the normalized frequency increases, peaks at some value of the normalized frequency and then decays. The normalized frequency that corresponds to the maximum group velocity shifts toward lower values as the core layer thickness increases. For d = 0.9 cm, the group velocity increases until it reaches 0.00506c at ω/ω_0 = 1.17225 GHz. For d = 1.0 cm, the group velocity reaches a maximum of 0.00409c at ω/ω_0 = 1.171 GHz. Finally, for d = 1.1 cm it reaches 0.00306c at ω/ω_0 = 1.16925 GHz. The group velocity shows

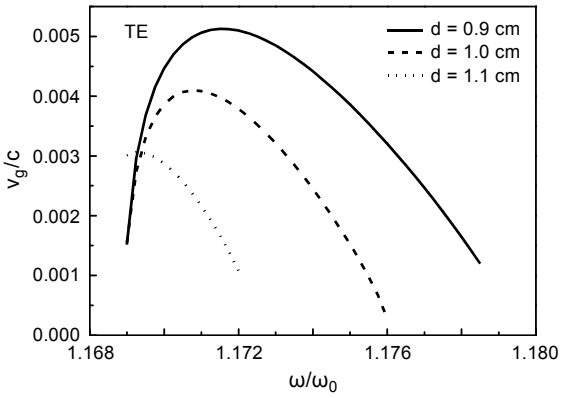

Fig. 6. Group velocity of surface waves *vs.* ω/ω_0 (TE) for different values of thickness of the guiding layer.

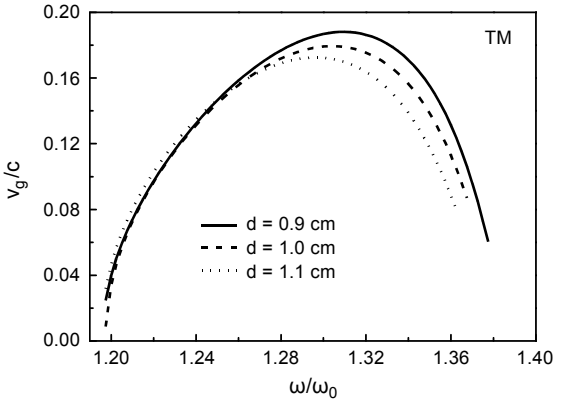

Fig. 7. Group velocity of surface waves *vs.* ω/ω_0 (TM) for different values of thickness of the guiding layer.

an almost linear dependence on wave frequency in some frequency bands. The group velocity of TM surface waves is shown in Fig. 7 for different core layer thickness. The same features observed in Fig. 6 are still available in Fig. 7. The group velocity increases with increasing ω/ω_0, peaks at optimum ω/ω_0 and then it decays. For $d = 0.9$ cm, $v_g = 0.1881$ at $\omega/\omega_0 = 1.31$ GHz. For thicknesses greater than 0.9 cm, the optimum ω/ω_0 at which the group velocity maximizes shows a shift towards smaller values.

4. Conclusion

Phase and group velocities of surface electromagnetic waves that propagate along the interface between the dielectric film and the left-handed material were investigated. The study reveals a normal dispersion property in which the effective index increases with the increase in the propagating wave frequency. As the core layer decreases, the dispersion curves move up showing an enhancement in the effective refractive index. It is found that the core layer thickness can be adjusted to broaden or narrow the operating

bands and modify the effective index to a desirable value. The operating frequency band for TM surface waves is much wider than that of TE surface waves. The phase velocity of surface TE wave shows a strong dependence on the wave frequency, especially for a large value of d. It decreases with increasing the frequency for both TE and TM surface waves. The phase velocity can be enhanced with the increase in the guiding layer thickness. The group velocity increases as the normalized frequency increases, peaks at some value of the normalized frequency and then decays. The normalized frequency that corresponds to the maximum group velocity shifts toward lower values as the core layer thickness increases.

References

[1] VESELAGO V.G., *The electrodynamics of substances with simultaneously negative values of ε and μ*, Soviet Physics Uspekhi **10**(4), 1968, pp. 509–514.

[2] PENDRY J.B., HOLDEN A.J., STEWART W.J., YOUNGS I., *Extremely low frequency plasmons in metallic mesostructures*, Physical Review Letters **76**(25), 1996, pp. 4773–4776.

[3] PENDRY J.B., *Negative refraction makes a perfect lens*, Physical Review Letters **85**(18), 2000, pp. 3966 –3969.

[4] RUPPIN R., *Surface polaritons of a left-handed material slab*, Journal of Physics: Condensed Matter **13**(9), 2001, pp. 1811–1819.

[5] ALU A., ENGHETA N., *Radiation from a traveling wave current sheet at the interface between a conventional material and a metamaterial with negative permittivity and permeability*, Microwave and Optical Technology Letters **35**(6), 2002, pp. 460–463.

[6] SHELBY R.A., SMITH D.R., NEMAT-NASSER S.C., SCHULTZ S., *Microwave transmission through a two -dimensional, isotropic, left-handed metamaterial*, Applied Physics Letters **78**(4), 2001, pp. 489–491.

[7] ENGHETA N., *An idea for thin subwavelength cavity resonators using metamaterials with negative permittivity and permeability*, IEEE Antennas and Wireless Propagation Letters **1**(1), 2002, pp. 10–13.

[8] MAHMOUD S.F., VIITANEN A.J., *Surface wave character on a slab of metamaterial with negative permittivity and permeability, progress in electromagnetics research*, Progress in Electromagnetics Research (PIER) **51**, 2005, pp. 127–137.

[9] LEI KANG, QIAN ZHAO, HONGJIE ZHAO, JI ZHOU, *Magnetically tunable negative permeability metamaterial composed by split ring resonators and ferrite rods*, Optics Express **16**(12), 2008, pp. 8825–8834.

[10] TAYA S.A., EL-FARRAM E.J., ABADLA M.M., *Symmetric multilayer slab waveguide structure with a negative index material: TM case*, Optik – International Journal for Light and Electron Optics **123**(24), 2012, pp. 2264–2268.

[11] ABADLA M., TAYA S., *Characteristics of left-handed multilayer slab waveguide structure*, The Islamic University Journal (Series of Natural Studies and Engineering) **19**, 2011, pp. 57–70.

[12] TAYA S.A., QADOURA I.M., *Guided modes in slab waveguides with negative index cladding and substrate*, Optik – International Journal for Light and Electron Optics **124**(13), 2013, pp. 1431–1436.

[13] TAYA S.A., QADOURA I.M., EL-WASIFE K.Y., *Scaling rules for a slab waveguide structure comprising nonlinear and negative index materials*, International Journal of Microwave and Optical Technology **7**(5), 2012, pp. 349–357.

[14] TAYA S.A., KULLAB H.M., QADOURA I.M., *Dispersion properties of slab waveguides with double negative material guiding layer and nonlinear substrate*, Journal of the Optical Society of America B **30**(7), 2013, pp. 2008–2013.

[15] HONG WEI YANG, HAIYAN SONG, *Symplectic FDTD method study left-handed material electromagnetic characteristics*, Optik – International Journal for Light and Electron Optics **124**(14), 2013, pp. 1716–1720.

[16] ZHENGPING WANG, ZHENHUI ZHANG, SHIMING QIN, LIHUI WANG, XIAOXIAO WANG, *Theoretical study on wave-absorption properties of a structure with left- and right-handed materials*, Materials and Design **29**(9), 2008, pp. 1777–1779.
[17] TAYA S.A., ELWASIFE K.Y., *Guided modes in a metal-clad waveguide comprising a left-handed material as a guiding layer*, International Journal of Research and Reviews in Applied Sciences (IJRRAS) **13**(1), 2012, pp. 294–305.
[18] TAYA S.A., ELWASIFE K.Y., KULLAB H.M., *Dispersion properties of anisotropic-metamaterial slab waveguide structure*, Optica Applicata **43**(4), 2013, pp. 857–869.
[19] ABADLA M., TAYA S., *Excitation of TE surface polaritons in different structures comprising a left-handed material and a metal*, Optik – International Journal for Light and Electron Optics **25**, 2014, pp. 1401–1405.
[20] VOSKOBOYNIKOV O., DYANKOV G., WIJERS C.M.J., *Left handed composite materials in the optical range*, Microelectronics Journal **36**(3–6), 2005, pp. 564–566.
[21] CHANGCHUN YAN, QIONG WANG, YIPING CUI, *Generating mechanism of the energy-stream loops for the evanescent waves in a left-handed material slab*, Optik – International Journal for Light and Electron Optics **121**(1), 2010, pp. 63–67.
[22] TAYA S.A., ELWASIFE K.Y., *Field profile of asymmetric slab waveguide structure with LHM layers*, Journal of Nano- and Electronic Physics **6**(2), 2014, article ID 02007.
[23] TAYA S.A., ALAMASSI D., *Reflection and transmission from left-handed material structures using Lorentz and Drude medium models*, Opto-Electronics Review **23**(3), 2015, pp. 214–221.
[24] HUANG C., CHEN D., WEI W.J., JING X.M., CHEN X., LIU J.Q., ZHU J., WEI Z.Y., LI H.Q., *A compact wide band filter based on the left handed material theory*, Microelectronic Engineering **85**(10), 2008, pp. 2183–2186.
[25] LAKHTAKIA A., *Positive and negative Goos–Hänchen shifts and negative phase-velocity mediums (alias left-handed materials)*, AEÜ – International Journal of Electronics and Communications **58**(3), 2004, pp. 229–231.
[26] TAYA S.A., *Slab waveguide with air core layer and anisotropic left-handed material claddings as a sensor*, Opto-Electronics Review **22**(4), 2014, pp. 252–257.
[27] TAYA S.A., *P-polarized surface waves in a slab waveguide with left-handed material for sensing applications*, Journal of Magnetism and Magnetic Materials **377**, 2015, pp. 281–285.
[28] TAYA S.A., *Theoretical investigation of slab waveguide sensor using anisotropic metamaterials*, Optica Applicata **45**(3), 2015, pp. 405–417.
[29] TAYA S.A., *Dispersion properties of lossy, dispersive, and anisotropic left-handed material slab waveguide*, Optik – International Journal for Light and Electron Optics **126**(14), 2015, pp. 1319–1323.
[30] KULLAB H.M., TAYA S.A., EL-AGEZ T.M., *Metal-clad waveguide sensor using a left-handed material as a core layer*, Journal of the Optical Society of America B **29**(5), 2012, pp. 959–964.
[31] KULLAB H.M., TAYA S.A., *Peak type metal-clad waveguide sensor using negative index materials*, AEÜ – International Journal of Electronics and Communications **67**(11), 2013, pp. 984–986.
[32] KULLAB H.M., TAYA S.A., *Transverse magnetic peak type metal-clad optical waveguide sensor*, Optik – International Journal for Light and Electron Optics **124**(24), 2013, pp. 7080–7084.
[33] TAYA S.A., KULLAB H.M., *Optimization of transverse electric peak-type metal-clad waveguide sensor using double-negative materials*, Applied Physics A **116**(4), 2014, pp. 1841–1846.
[34] KULLAB H.M., QADOURA I.M., TAYA S.A., *Slab waveguide sensor with left-handed material core layer for detection an adlayer thickness and index*, Journal of Nano- and Electronic Physics **7**(2), 2015, article ID 02039.

Received July 21, 2016
in revised form October 1, 2016